

A POSTERIORI ERROR ESTIMATION FOR PARABOLIC PROBLEMS WITH DYNAMIC BOUNDARY CONDITIONS

R. ALTMANN[†], C. ZIMMER[†]

ABSTRACT. This paper is concerned with adaptive mesh refinement strategies for the spatial discretization of parabolic problems with dynamic boundary conditions. This includes the characterization of inf–sup stable discretization schemes for a stationary model problem as a preliminary step. Based on an alternative formulation of the system as a partial differential–algebraic equation, we introduce a posteriori error estimators which allow local refinements as well as a special treatment of the boundary. We prove reliability and efficiency of the estimators and illustrate their performance in several numerical experiments.

Key words. dynamic boundary conditions, adaptivity, PDAE, parabolic PDE

AMS subject classifications. 65M60, 65L80, 65J10

1. INTRODUCTION

Within this paper, we consider a linear parabolic model problem with so-called *dynamic boundary conditions* in a bounded Lipschitz domain $\Omega \subseteq \mathbb{R}^d$, $d \in \{2, 3\}$, on a time horizon $[0, T]$, $0 < T < \infty$, namely

$$(1.1a) \quad \dot{u} - \Delta_\alpha u = \hat{f} \quad \text{in } \Omega,$$

$$(1.1b) \quad \dot{u} - \Delta_{\Gamma, \kappa} u + \partial_{\alpha, \nu} u = \hat{g} \quad \text{on } \Gamma := \partial\Omega$$

with initial condition $u(0) = u^0$ and sufficiently smooth right-hand sides \hat{f} , \hat{g} . Therein, we write

$$\Delta_\alpha u := \nabla \cdot (\alpha \nabla u), \quad \Delta_{\Gamma, \kappa} u := \nabla_\Gamma \cdot (\kappa \nabla_\Gamma u)$$

for the weighted Laplacians with uniformly positive diffusion coefficients $\alpha \in L^\infty(\Omega)$ and $\kappa \in L^\infty(\Gamma)$. In the special case $\kappa \equiv 1$, the differential operator in (1.1b) equals the well-known Laplace–Beltrami operator; see [GT01, Ch. 16.1]. Moreover, $\partial_{\alpha, \nu} u := \nu \cdot (\alpha \nabla u)$ denotes the normal derivative corresponding to the differential operator in (1.1a) with unit normal vector ν .

Condition (1.1b) itself is a differential equation and enables the reflection of effective properties on the boundary of the domain [Esc93, Gol06]. To be more precise, this means that the momentum on the boundary is taken into account during the modeling process rather than being neglected as for standard boundary conditions. Because of this flexibility, this and similar models have attained increasing popularity nowadays, cf. [Gol06, Vit18, LW19]. Although well-understood from a theoretical point (see, e.g., [FGGR02, VV08]), results on the numerical approximation of such systems are still limited [VS13, KL17].

Date: February 7, 2023.

Both authors acknowledge the support of the Deutsche Forschungsgemeinschaft (DFG, German Research Foundation) through the project 446856041.

Within this paper, we benefit from a special formulation of (1.1) as *partial differential–algebraic equation* (PDAE); see [LMT13, Alt15] for an introduction. This means that we interpret the equations as a coupled system with an additional variable acting only on the boundary; see [Las02, Ch. 5.3] as well as [Alt19]. The resulting PDAE approach has already proven advantageous from a numerical point of view in the context of heterogeneous boundary conditions [AV21], phase separation models such as the Cahn–Hilliard equation [AZ22a], and the design of bulk–surface splitting schemes [AKZ22, AZ22b, CFK23]. The main instrument of the PDAE approach is the possibility to apply different discretization schemes in the bulk Ω and on the boundary Γ , e.g., based on different meshes \mathcal{T}_Ω and \mathcal{T}_Γ . This is also exploited in the present paper and is of special interest in applications where the solution oscillates rapidly on the boundary. Such oscillations also call for adaptive mesh refinements in order to improve the computational efficiency. Adaptive strategies, on the other hand, are based on a posteriori error estimates, which were first introduced for elliptic problems; see [AO97, Lip04, Ver13].

The paper is structured as follows. After the introduction of the PDAE model in Section 2.1, we shortly consider the temporal discretization and introduce a stationary model problem with a saddle point structure. Afterwards, we discuss inf–sup stable finite element schemes for this model problem in Section 2.3. Based on classical finite element literature, we construct (local) a posteriori error estimators in Section 3. Of special emphasis is the possibility to distinguish needed refinements of the bulk mesh on the boundary (denoted by $\mathcal{T}_\Omega|_\Gamma$) and the boundary mesh \mathcal{T}_Γ . Moreover, we prove that these estimators are reliable as well as efficient, meaning that the estimators are indeed in the range of the actual error. We complete the paper with a number of numerical experiments in Section 4. This includes stationary problems on different spatial domains but also a dynamic problem such as (1.1).

Notation. Throughout the paper we write $a \lesssim b$ to indicate that there exists a generic constant C , independent of any spatial and temporal discretization parameters, such that $a \leq Cb$.

2. WEAK FORMULATION AND DISCRETIZATION

In this preliminary section, we introduce the weak operator formulation of the model problem (1.1) in PDAE form. Moreover, we discuss the discretization in time and space.

2.1. Weak formulation. With the introduction of an auxiliary variable $p := \text{tr } u$ (with tr denoting the usual trace operator) as proposed in [Alt19] and the spaces

$$\mathcal{V} := H^1(\Omega), \quad \mathcal{Q} := H^1(\Gamma), \quad \mathcal{M} := H^{-1/2}(\Gamma),$$

the weak form of (1.1) can be expressed as the following PDAE: Find $u: [0, T] \rightarrow \mathcal{V}$, $p: [0, T] \rightarrow \mathcal{Q}$, and a Lagrange multiplier $\lambda: [0, T] \rightarrow \mathcal{M}$ such that

$$(2.1a) \quad \begin{bmatrix} \dot{u} \\ \dot{p} \end{bmatrix} + \begin{bmatrix} \mathcal{K}_u & \\ & \mathcal{K}_p \end{bmatrix} \begin{bmatrix} u \\ p \end{bmatrix} + \begin{bmatrix} -\mathcal{B}_u^* \\ \mathcal{B}_p^* \end{bmatrix} \lambda = \begin{bmatrix} \hat{f} \\ \hat{g} \end{bmatrix} \quad \text{in } (\mathcal{V} \times \mathcal{Q})^*,$$

$$(2.1b) \quad \mathcal{B}_u u - \mathcal{B}_p p = 0 \quad \text{in } \mathcal{M}^*.$$

This formulation includes the differential operators $\mathcal{K}_u: \mathcal{V} \rightarrow \mathcal{V}^*$ and $\mathcal{K}_p: \mathcal{Q} \rightarrow \mathcal{Q}^*$ given by

$$\langle \mathcal{K}_u u, v \rangle := \int_\Omega \alpha \nabla u \cdot \nabla v \, dx, \quad \langle \mathcal{K}_p p, q \rangle := \int_\Gamma \kappa \nabla_\Gamma p \cdot \nabla_\Gamma q \, dx$$

as well as the trace operator $\mathcal{B}_u: \mathcal{V} \rightarrow \mathcal{M}^*$ and the canonical embedding $\mathcal{B}_p: \mathcal{Q} \rightarrow \mathcal{M}^*$.

We would like to emphasize that (2.1) depicts an extended formulation where the connection of u and its trace p is explicitly stated in the form of a constraint. In contrast to the classical formulation (1.1), the PDAE (2.1) includes a Lagrange multiplier as additional variable which satisfies $\lambda = \partial_{\alpha,\nu} u$ if the solution is sufficiently smooth. Moreover, the system comes together with initial data $u(0) = u^0$ and $p(0) = p^0$, which is called *consistent* if they coincide on the boundary, i.e., if $\mathcal{B}_u u^0 = \mathcal{B}_p p^0$.

At this point, we would like to emphasize that a direct spatial discretization of (2.1) leads to a differential–algebraic equation (of differentiation index 2). In general, this implies numerical difficulties within the temporal discretization, cf. [HLR89, HW96]. Since the right-hand side of the constraint (2.1b) is homogeneous, however, these instabilities do not occur for consistent initial values and an index reduction is not needed, cf. [HLR89, p. 33].

Within this paper, we follow the *Rothe method* for the discretization of system (2.1), i.e., we first discretize in time and then in space. The time discretization is shortly discussed in the following subsection, whereas we will focus on the spatial discretization using adaptive finite elements in each time step in Section 2.3.

2.2. Temporal discretization. We first consider the application of the implicit Euler scheme to (2.1) with constant step size τ . Given approximations $u^n \in \mathcal{V}$ and $p^n \in \mathcal{Q}$ of u and p at time point $t^n := n\tau$, respectively, we seek $u^{n+1} \in \mathcal{V}$, $p^{n+1} \in \mathcal{Q}$, and $\lambda^{n+1} \in \mathcal{M}$ as the solution of

$$(2.2a) \quad \begin{bmatrix} u^{n+1} \\ p^{n+1} \end{bmatrix} + \begin{bmatrix} \tau\mathcal{K}_u & \\ & \tau\mathcal{K}_p \end{bmatrix} \begin{bmatrix} u^{n+1} \\ p^{n+1} \end{bmatrix} + \begin{bmatrix} -\tau\mathcal{B}_u^* \\ \tau\mathcal{B}_p^* \end{bmatrix} \lambda^{n+1} = \begin{bmatrix} \tilde{f} \\ \tilde{g} \end{bmatrix} \quad \text{in } (\mathcal{V} \times \mathcal{Q})^*,$$

$$(2.2b) \quad \mathcal{B}_u u^{n+1} - \mathcal{B}_p p^{n+1} = 0 \quad \text{in } \mathcal{M}^*.$$

Therein, \tilde{f} (and similarly \tilde{g}) is some right-hand side which depends the previous approximation u^n (respectively p^n).

Remark 2.1. For semilinear applications, i.e., if we allow f and g to depend on u and p , respectively, we obtain the same linear structure as long as the nonlinear terms are treated *explicitly*.

In summary, an implicit Euler discretization leads to the following (stationary) problem, which needs to be solved in every time step: Given $f \in \mathcal{V}^*$ and $g \in \mathcal{Q}^*$, find $u \in \mathcal{V}$, $p \in \mathcal{Q}$, and $\lambda \in \mathcal{M}$ such that

$$\begin{bmatrix} u \\ p \end{bmatrix} + \begin{bmatrix} \tau\mathcal{K}_u & \\ & \tau\mathcal{K}_p \end{bmatrix} \begin{bmatrix} u \\ p \end{bmatrix} + \begin{bmatrix} -\tau\mathcal{B}_u^* \\ \tau\mathcal{B}_p^* \end{bmatrix} \lambda = \begin{bmatrix} f \\ g \end{bmatrix} \quad \text{in } (\mathcal{V} \times \mathcal{Q})^*,$$

$$\mathcal{B}_u u - \mathcal{B}_p p = 0 \quad \text{in } \mathcal{M}^*.$$

This motivates the model problem, which we will consider in Section 3, namely

$$(2.3a) \quad (\sigma - \Delta_\alpha) u = f,$$

$$(2.3b) \quad (\sigma - \Delta_{\Gamma,\kappa}) p + \lambda = g,$$

$$(2.3c) \quad \text{tr } u - p = 0.$$

Note that this model is written in its strong form because of which the Lagrange multiplier (being equal to the weighted normal trace) disappears in the first equation. Moreover, the

newly introduced parameter $\sigma > 0$ corresponds to τ^{-1} in the case of an implicit Euler discretization.

Remark 2.2 (Discretization by Runge–Kutta methods). Assume a Butcher tableau

$$\begin{array}{c|c} \mathbf{c} & \mathbf{A} \\ \hline & \mathbf{b}^T \end{array}$$

with an invertible coefficient matrix $\mathbf{A} \in \mathbb{R}^{s,s}$, which defines an algebraically stable Runge–Kutta scheme. According to [Zim21, Sect. 8.3 f.], this leads to a stable approximation. Furthermore, we assume that $-\mathbf{A}$ is globally stable, which is equivalent to the existence of a symmetric matrix $\mathbf{D} \in \mathbb{R}^{s,s}$ such that \mathbf{D} and $\mathbf{D}\mathbf{A}^{-1} + \mathbf{A}^{-T}\mathbf{D}$ are positive definite [LT85, Th. 13.1.1]. Then, the calculation of the internal stages $\mathbf{u}^{n+1} \in \mathcal{V}^s$, $\mathbf{p}^{n+1} \in \mathcal{Q}^s$, $\boldsymbol{\lambda}^{n+1} \in \mathcal{M}^s$ can be treated similarly to the implicit Euler method considered above. In comparison to (2.2), u^{n+1} (and analogously p^{n+1} and λ^{n+1}) needs to be replaced by \mathbf{u}^{n+1} . The operators are replaced by their Kronecker product with \mathbf{D} , e.g., \mathcal{K} turns into $\mathbf{D} \otimes \mathcal{K}$. Moreover, the operator $\mathbf{D}\mathbf{A}^{-1} \otimes \text{id}$ pops up in front of \mathbf{u}^{n+1} and \mathbf{p}^{n+1} . Finally, \tilde{f} (and analogously \tilde{g}) contains the approximation of the previous time point $u^n = (1 - \mathbf{b}^T \mathbf{A}^{-1} \mathbf{e})u^{n-1} + \mathbf{b}^T \mathbf{A}^{-1} \mathbf{u}^n$, $n = 1, 2, \dots$, with $\mathbf{e} = [1, \dots, 1]^T \in \mathbb{R}^s$; cf. [Zim21, Ch. 5 & 8].

For the translation of the upcoming analysis given in Section 3 to the Runge–Kutta case, one uses that the assumptions on the matrix \mathbf{D} imply

$$\begin{aligned} \|\mathbf{u}^{n+1}\|_{[L^2(\Omega)]^s}^2 &\lesssim (\mathbf{D}\mathbf{A}^{-1}\mathbf{u}^{n+1}, \mathbf{u}^{n+1})_{[L^2(\Omega)]^s} \lesssim \|\mathbf{u}^{n+1}\|_{[L^2(\Omega)]^s}^2, \\ |\mathbf{u}^{n+1}|_{[H^1(\Omega)]^s}^2 &\lesssim \langle (\mathbf{D} \otimes \mathcal{K}_u)\mathbf{u}^{n+1}, \mathbf{u}^{n+1} \rangle \lesssim |\mathbf{u}^{n+1}|_{[H^1(\Omega)]^s}^2. \end{aligned}$$

Examples of diagonal matrices \mathbf{D} for the Gauss–Legendre, Radau IA, and Radau IIA methods can be found at [HW96, p. 220 f.].

2.3. Stable spatial discretization. We first collect a number of standard finite element spaces, which will be used in the following. Given a regular triangulation \mathcal{T}_Ω of the computational domain Ω , the space of (discontinuous) piecewise polynomials of degree $k \geq 0$ is denoted by

$$\mathcal{P}_k^d(\mathcal{T}_\Omega) := \{v \in L^2(\Omega) \mid v|_T \text{ is a polynomial of degree } \leq k \text{ for all } T \in \mathcal{T}_\Omega\}.$$

The subspace of functions which are additionally elements of $H^1(\Omega)$, is denoted by $\mathcal{P}_k(\mathcal{T}_\Omega)$. It is well-known that this space can be characterized by

$$\mathcal{P}_k(\mathcal{T}_\Omega) = \mathcal{P}_k^d(\mathcal{T}_\Omega) \cap C(\Omega);$$

see, e.g., [Bra07, Th. II.5.2]. Given a regular triangulation \mathcal{T}_Γ of the boundary Γ we denote analogously the space of (possibly discontinuous) piecewise polynomial functions and its subspace of continuous functions by $\mathcal{P}_k^d(\mathcal{T}_\Gamma)$ and $\mathcal{P}_k(\mathcal{T}_\Gamma)$, respectively.

For the construction of stable finite element schemes, we further introduce the space of *bubble functions*. In two space dimensions, the edge-bubble function ψ_E equals the scaled product of the two nodal basis functions corresponding to the nodes of the edge E . For $d = 3$, ψ_E denotes the face-bubble (E being a face in \mathcal{T}_Ω) and equals the scaled product of the three corresponding nodal basis functions, cf. [Ver13]. This leads to the space

$$\begin{aligned} \mathcal{E}_\ell(\mathcal{T}_\Omega) &:= \{v \cdot \psi_E \mid v|_T \text{ is a polynomial of degree } \leq \ell \text{ for all } T \in \mathcal{T}_\Omega, \\ &\quad \psi_E \text{ is an edge/face-bubble for } E \subseteq \Gamma\} \subseteq P_{\ell+d}(\mathcal{T}_\Omega). \end{aligned}$$

Now let \mathbb{V}_h , \mathbb{Q}_h , and \mathbb{M}_h denote finite-dimensional subspaces of \mathcal{V} , \mathcal{Q} , and \mathcal{M} . Due to the saddle point structure of the model problem, these spaces need to satisfy a discrete inf-sup condition, which reads

$$(2.4) \quad \inf_{\lambda_h \in \mathbb{M}_h \setminus \{0\}} \sup_{(u_h, p_h) \in \mathbb{V}_h \times \mathbb{Q}_h \setminus \{0\}} \frac{\langle \mathcal{B}_u u_h - \mathcal{B}_p p_h, \lambda_h \rangle_\Gamma}{\|\lambda_h\|_{\mathcal{M}} (\|u_h\|_{\mathcal{V}}^2 + \|p_h\|_{\mathcal{Q}}^2)^{1/2}} \geq \beta > 0$$

for some positive constant β being independent of the mesh sizes. Here, $\langle \cdot, \cdot \rangle_\Gamma$ denotes the dual product in \mathcal{M} , which only acts on Γ . In a first result, we show that this stability condition is independent of the choice of the space \mathbb{Q}_h .

Theorem 2.3 (Equivalence of inf-sup stable discretizations). *Consider a conforming Galerkin scheme $\mathbb{V}_h \subseteq \mathcal{V} = H^1(\Omega)$, $\mathbb{Q}_h \subseteq \mathcal{Q} = H^1(\Gamma)$, and $\mathbb{M}_h \subseteq \mathcal{M} = H^{-1/2}(\Gamma)$, which includes the approximation property of the family \mathbb{V}_h . Then, the discrete inf-sup condition (2.4) is satisfied if and only if there exists a positive constant $\hat{\beta}$ (independent of the mesh size) such that*

$$(2.5) \quad \inf_{\lambda_h \in \mathbb{M}_h \setminus \{0\}} \sup_{u_h \in \mathbb{V}_h \setminus \{0\}} \frac{\langle \mathcal{B}_u u_h, \lambda_h \rangle_\Gamma}{\|\lambda_h\|_{\mathcal{M}} \|u_h\|_{\mathcal{V}}} \geq \hat{\beta} > 0.$$

Proof. (\Rightarrow) We prove the if-part by contrapositive and assume that (2.5) is not satisfied. Then, there exists a sequence $\{\lambda_h^*\} \subseteq \mathcal{M}$ with $\lambda_h^* \in \mathbb{M}_h$ and $\|\lambda_h^*\|_{\mathcal{M}} = 1$ such that

$$a_h := \sup_{u_h \in \mathbb{V}_h \setminus \{0\}} \frac{\langle \mathcal{B}_u u_h, \lambda_h^* \rangle_\Gamma}{\|u_h\|_{\mathcal{V}}} \rightarrow 0 \quad \text{as } h \rightarrow 0^+.$$

Since the sequence is uniformly bounded, there exists a subsequence h' of h with $\lambda_{h'}^* \rightharpoonup \lambda^*$ in \mathcal{M} as $h' \rightarrow 0^+$. Let $g \in \mathcal{M}^* \setminus \{0\}$ be arbitrary. The surjectivity of $\mathcal{B}_u \in \mathcal{L}(\mathcal{V}, \mathcal{M}^*)$, [Bra07, Ch. III, Th. 4.2], implies the existence of a $u \in \mathcal{V}$ with $\mathcal{B}_u u = g$. Due to the assumed approximation property of \mathbb{V}_h , there exists a sequence $\{u_h\}_h \subseteq \mathcal{V}$ with $u_h \in \mathbb{V}_h$, $u_h \neq 0$, and $\lim_{h \rightarrow 0^+} u_h = u$ in \mathcal{V} . By the strong convergence of $\{u_h\}_h$ and the weak convergence of $\{\lambda_{h'}^*\}_{h'}$, we have

$$0 \leq |\langle g, \lambda^* \rangle_\Gamma| = \lim_{h' \rightarrow 0^+} |\langle \mathcal{B}_u u_{h'}, \lambda_{h'}^* \rangle_\Gamma| = \lim_{h' \rightarrow 0^+} \|u\|_{\mathcal{V}} \frac{|\langle \mathcal{B}_u u_{h'}, \lambda_{h'}^* \rangle_\Gamma|}{\|u_{h'}\|_{\mathcal{V}}} \leq \lim_{h' \rightarrow 0^+} \|u\|_{\mathcal{V}} a_{h'} = 0.$$

Hence, $\lambda^* = 0$ holds and the entire sequence $\{\lambda_h^*\}$ vanishes weakly in $\mathcal{M} = H^{-1/2}(\Gamma)$, cf. [GGZ74, Ch. I, Lem. 5.4]. Moreover, the sequence vanishes strongly in $\mathcal{Q}^* = H^{-1}(\Gamma)$, since the weak limit is unique and the embedding $H^{-1/2}(\Gamma) \hookrightarrow H^{-1}(\Gamma)$ is compact [Tay11, Prop. 3.2 & 3.4]. Finally, this leads to

$$\begin{aligned} & \lim_{h \rightarrow 0^+} \inf_{\lambda_h \in \mathbb{M}_h \setminus \{0\}} \sup_{(u_h, p_h) \in \mathbb{V}_h \times \mathbb{Q}_h \setminus \{0\}} \frac{\langle \mathcal{B}_u u_h - \mathcal{B}_p p_h, \lambda_h \rangle_\Gamma}{\|\lambda_h\|_{\mathcal{M}} (\|u_h\|_{\mathcal{V}}^2 + \|p_h\|_{\mathcal{Q}}^2)^{1/2}} \\ & \leq \lim_{h \rightarrow 0^+} \sup_{(u_h, p_h) \in \mathbb{V}_h \times \mathbb{Q}_h \setminus \{0\}} \frac{\langle \mathcal{B}_u u_h - \mathcal{B}_p p_h, \lambda_h^* \rangle_\Gamma}{(\|u_h\|_{\mathcal{V}}^2 + \|p_h\|_{\mathcal{Q}}^2)^{1/2}} \\ & \leq \lim_{h \rightarrow 0^+} \sup_{u_h \in \mathbb{V}_h \setminus \{0\}} \frac{\langle \mathcal{B}_u u_h, \lambda_h^* \rangle_\Gamma}{\|u_h\|_{\mathcal{V}}} + \sup_{p_h \in \mathbb{Q}_h \setminus \{0\}} \frac{\langle \mathcal{B}_p p_h, \lambda_h^* \rangle_\Gamma}{\|p_h\|_{\mathcal{Q}}} \\ & \leq \lim_{h \rightarrow 0^+} a_h + \|\lambda_h^*\|_{\mathcal{Q}^*} = 0, \end{aligned}$$

where we have used that \mathcal{B}_p is the embedding operator of $\mathcal{Q} = H^1(\Gamma)$ into $\mathcal{M}^* = H^{1/2}(\Gamma)$. Thus, the inf-sup expression cannot be bounded uniformly from below by a $\beta > 0$.

(\Leftarrow) The only-if-part follows immediately by

$$\sup_{(u_h, p_h) \in \mathbb{V}_h \times \mathbb{Q}_h \setminus \{0\}} \frac{\langle \mathcal{B}_u u_h - \mathcal{B}_p p_h, \lambda_h \rangle_\Gamma}{(\|u_h\|_{\mathbb{V}}^2 + \|p_h\|_{\mathbb{Q}}^2)^{1/2}} \geq \sup_{u_h \in \mathbb{V}_h \setminus \{0\}} \frac{\langle \mathcal{B}_u u_h, \lambda_h \rangle_\Gamma}{\|u_h\|_{\mathbb{V}}} \geq \hat{\beta} \|\lambda_h\|_{\mathcal{M}}. \quad \square$$

Remark 2.4. In the limit case $\kappa \equiv 0$, there is no differential operator acting on the boundary and the boundary conditions are called *locally reacting*. The corresponding solution spaces then read $\mathcal{V} = H^1(\Omega)$, $\mathcal{Q} = L^2(\Gamma)$, and $\mathcal{M} = L^2(\Gamma)$. In this setting, one can show analogously to Theorem 2.3 that conforming finite element spaces are inf-sup stable if and only if the subproblem with $\mathbb{V}_h = \{0\}$ is inf-sup stable.

A direct consequence of Theorem 2.3 is that it is sufficient to consider the inf-sup condition with $p_h = 0$. Hence, one example class of inf-sup stable discretizations reads

$$\mathbb{V}_h := \mathcal{P}_k(\mathcal{T}_\Omega) \oplus \mathcal{E}_\ell(\mathcal{T}_\Omega) \subseteq \mathcal{V}, \quad \mathbb{Q}_h \subseteq \mathcal{Q}, \quad \mathbb{M}_h := \mathcal{P}_\ell^d(\mathcal{T}_\Omega|_\Gamma) \subseteq \mathcal{M}$$

with $k \geq 1$, $\ell \geq 0$; see [Lip04, Th. 2.3.7]. We would like to emphasize that the mesh used for the definition of \mathbb{M}_h may be different to $\mathcal{T}_\Omega|_\Gamma$ as long as it is synchronized with the mesh used for the bubble functions. Moreover, the scheme

$$\mathbb{V}_h := \mathcal{P}_1(\mathcal{T}_\Omega) \subseteq \mathcal{V}, \quad \mathbb{Q}_h \subseteq \mathcal{Q}, \quad \mathbb{M}_h := \mathcal{P}_1(\mathcal{T}_\Omega|_\Gamma) \subseteq \mathcal{M}$$

is inf-sup stable; see [AV21, Prop. 3.4]. The corresponding generalization to higher polynomial degrees reads as follows.

Lemma 2.5. *The conforming finite element spaces*

$$\mathbb{V}_h := \mathcal{P}_k(\mathcal{T}_\Omega) \subseteq \mathcal{V}, \quad \mathbb{Q}_h \subseteq \mathcal{Q}, \quad \mathbb{M}_h := \mathcal{P}_k(\mathcal{T}_\Omega|_\Gamma) \subseteq \mathcal{M}$$

satisfy the discrete inf-sup condition (2.4) for arbitrary $k \geq 1$ and \mathbb{Q}_h .

Proof. The case $k = 1$ is shown in [AV21, Prop. 3.4]. The statement for general k can be proven equivalently. Here, we use that there exists an extension operator from $\mathcal{P}_k(\mathcal{T}_\Omega|_\Gamma) \subseteq H^{1/2}(\Omega)$ to $\mathcal{P}_k(\mathcal{T}_\Omega) \subseteq H^1(\Omega)$ which is continuous and preserves boundary values; cf. [HM12, Lem. 5.1] and [SZ90, Th. 2.1]. In particular, its operator-norm depends only on Ω and the regularity of the triangulation \mathcal{T}_Ω . \square

Recall that all presented stable schemes still have the freedom to set the discrete space \mathbb{Q}_h . In the following, \mathbb{Q}_h will be a standard finite element space but defined on another triangulation \mathcal{T}_Γ . Having in mind applications with strong fluctuations or heterogeneities on the boundary, \mathcal{T}_Γ usually equals a refinement of $\mathcal{T}_\Omega|_\Gamma$.

3. A POSTERIORI ERROR ESTIMATION

After the discussion on the temporal discretization and inf-sup stable finite element schemes, we now turn to the construction of efficient and reliable a posteriori error estimators. Following the Rothe method, the aim is an adaptive spatial discretization in each time step. Note that the formulation as coupled system in (2.1) amplifies the use of adaptive schemes as we can optimize \mathcal{T}_Ω (for the spaces $\mathbb{V}_h, \mathbb{M}_h$) as well as \mathcal{T}_Γ (for \mathbb{Q}_h). Throughout this paper, we assume \mathcal{T}_Ω and \mathcal{T}_Γ to be shape regular. Note that this automatically implies the shape regularity (and quasi-uniformity) of $\mathcal{T}_\Omega|_\Gamma$. Within this section, we consider the two-dimensional setting but comment on necessary adjustments in the three-dimensional case.

By \mathcal{E}_Ω we denote the set of edges corresponding to the triangulation \mathcal{T}_Ω , which can be decomposed into $\mathcal{E}_\Omega^{\text{in}}$ (interior edges) and $\mathcal{E}_\Omega^{\text{bd}}$ (boundary edges). Moreover, h_T , h_I , and h_E denote the mesh sizes for elements and edges of a triangulation, respectively. For the upcoming analysis, we consider the following assumption.

Assumption 3.1 (Spatial discretization).

- (1) The discretization scheme is inf-sup stable and it holds that $\mathcal{P}_1(\mathcal{T}_\Omega) \subseteq \mathbb{V}_h$, $\mathcal{P}_1(\mathcal{T}_\Gamma) \subseteq \mathbb{Q}_h$, and $\mathcal{P}_1(\mathcal{T}_\Omega|_\Gamma) \subseteq \mathbb{M}_h$ or $\mathcal{P}_0^{\text{d}}(\mathcal{T}_\Omega|_\Gamma) \subseteq \mathbb{M}_h$.
- (2) \mathcal{T}_Γ is a refinement of $\mathcal{T}_\Omega|_\Gamma$. Moreover, there exists a positive constant $\rho > 0$ such that $h_E \leq \rho h_I$ holds uniformly for every $I \in \mathcal{T}_\Gamma$ with $I \subseteq E \in \mathcal{E}_\Omega^{\text{bd}}$.
- (3) The diffusion coefficients satisfy $\alpha \in \mathcal{P}_1^{\text{d}}(\mathcal{T}_\Omega)$ and $\kappa \in \mathcal{P}_1^{\text{d}}(\mathcal{T}_\Gamma)$.

As explained in Section 2.2, we deal with the model problem (2.3). Working again with the weak form, we consider the system

$$\begin{aligned} \sigma(u, v)_{L^2(\Omega)} + \langle \mathcal{K}_u u, v \rangle - \langle \lambda, v \rangle_\Gamma &= (f, v)_{L^2(\Omega)}, \\ \sigma(p, q)_{L^2(\Gamma)} + \langle \mathcal{K}_p p, q \rangle + \langle \lambda, q \rangle_\Gamma &= (g, q)_{L^2(\Gamma)}, \\ \langle u - p, \mu \rangle_\Gamma &= 0 \end{aligned}$$

for test functions $v \in \mathcal{V}$, $q \in \mathcal{Q}$, $\mu \in \mathcal{M}$ and the parameter σ which is related to the time step size.

Remark 3.2. The upcoming analysis can be performed similarly for semilinear applications; see [Ver13, Sect. 5.2.3]. We, however, focus on the linear case, since our main interest is the treatment of the two different meshes on the boundary.

To shorten notation, we define the product space $\mathcal{X} := \mathcal{V} \times \mathcal{Q} \times \mathcal{M}$ equipped with the norm

$$\|[u, p, \lambda]\|^2 := \|u\|_{\mathcal{V}}^2 + \|p\|_{\mathcal{Q}}^2 + \|\lambda\|_{\mathcal{M}}^2.$$

Moreover, we introduce the bilinear form $B: \mathcal{X} \times \mathcal{X} \rightarrow \mathbb{R}$, which is directly related to the model problem, by

$$\begin{aligned} B([u, p, \lambda], [v, q, \mu]) &= \int_{\Omega} \sigma uv + \alpha \nabla u \cdot \nabla v \, dx + \int_{\Gamma} \sigma pq + \kappa \nabla_{\Gamma} p \cdot \nabla_{\Gamma} q \, ds + \int_{\Gamma} (u - p)\mu - (v - q)\lambda \, ds. \end{aligned}$$

Note that we use the symbolic integral notation for the boundary terms as they equal the L^2 -inner product if the arguments are sufficiently smooth. Obviously, the bilinear form B is continuous. Furthermore, following the lines of [Ver13, Prop. 4.68], one can show that B is inf-sup stable, i.e., there exists a positive constant $\beta_B > 0$ such that

$$(3.1) \quad \sup_{[v, q, \mu] \in \mathcal{X}, \|[v, q, \mu]\|=1} B([u, p, \lambda], [v, q, \mu]) \geq \beta_B \|[u, p, \lambda]\|.$$

With B at hand, the introduced weak form of the model problem can be written as

$$B([u, p, \lambda], [v, q, \mu]) = \int_{\Omega} f v \, dx + \int_{\Gamma} g q \, ds$$

for all $[v, q, \mu] \in \mathcal{X}$. Correspondingly, given discrete spaces $\mathbb{V}_h \subset \mathcal{V}$, $\mathbb{Q}_h \subset \mathcal{Q}$, and $\mathbb{M}_h \subset \mathcal{M}$ and the product space $\mathbb{X}_h := \mathbb{V}_h \times \mathbb{Q}_h \times \mathbb{M}_h$, we obtain a discrete solution triple $[u_h, p_h, \lambda_h] \in \mathbb{X}_h$ as the unique solution of

$$B([u_h, p_h, \lambda_h], [v_h, q_h, \mu_h]) = \int_{\Omega} f v_h \, dx + \int_{\Gamma} g q_h \, ds$$

for all $[v_h, q_h, \mu_h] \in \mathbb{X}_h$. Standard arguments such as in [BF91, Sect. II.2.2] imply the a priori estimate

$$\| [u - u_h, p - p_h, \lambda - \lambda_h] \| \lesssim \inf_{[v_h, q_h, \mu_h] \in \mathbb{X}_h} \| u - v_h \|_{H^1(\Omega)} + \| p - q_h \|_{H^1(\Gamma)} + \| \lambda - \mu_h \|_{H^{-1/2}(\Gamma)}.$$

At this point, we would like to recall that we are especially interested in cases where strong fluctuations occur on the boundary. This means, in particular, that we expect \mathbb{Q}_h to be a refinement of \mathbb{V}_h restricted to the boundary. Moreover, this motivates the use of adaptive methods, which are based on a posteriori error estimates. These are topic of the upcoming subsection.

3.1. Construction of local estimators. Following the methodology of [Lip04, Ver13], we aim to construct a posteriori error estimators which can distinguish necessary refinements for the approximations of $u|_\Gamma$ and p , respectively. Within this section, the triple $[u, p, \lambda] \in \mathcal{X}$ denotes the weak solution to the model problem (2.3) and $[u_h, p_h, \lambda_h] \in \mathbb{X}_h$ its discrete counterpart. As a consequence of (3.1), we have the error bound

$$\begin{aligned} \| u - u_h \|_{H^1(\Omega)} + \| p - p_h \|_{H^1(\Gamma)} + \| \lambda - \lambda_h \|_{H^{-1/2}(\Gamma)} \\ \leq \frac{\sqrt{3}}{\beta_B} \sup_{[v, q, \mu] \in \mathcal{X}, \| [v, q, \mu] \| = 1} B([u - u_h, p - p_h, \lambda - \lambda_h], [v, q, \mu]). \end{aligned}$$

In order to bound the right-hand side, we integrate by parts and obtain

$$\begin{aligned} & B([u - u_h, p - p_h, \lambda - \lambda_h], [v, q, \mu]) \\ &= \sum_{T \in \mathcal{T}_\Omega} \int_T (f - \sigma u_h + \Delta_\alpha u_h) v \, dx - \sum_{E \in \mathcal{E}_\Omega^{\text{in}}} \int_E [\alpha \nabla u_h \cdot n_E]_E v \, ds \\ &+ \sum_{E \in \mathcal{E}_\Omega^{\text{bd}}} \int_E (\lambda_h - \alpha \nabla u_h \cdot n_E) v \, ds + \sum_{I \in \mathcal{T}_\Gamma} \int_I (g - \sigma p_h + \Delta_{\Gamma, \kappa} p_h - \lambda_h) q \, ds \\ &- \sum_{x \in \mathcal{N}_\Gamma} [\kappa \nabla_\Gamma p_h]_x q(x) - \int_\Gamma (u_h - p_h) \mu \, ds \end{aligned}$$

for every $[v, q, \mu] \in \mathcal{X}$. Recall that $\mathcal{E}_\Omega^{\text{in}}$ and $\mathcal{E}_\Omega^{\text{bd}}$ denote the set of interior and boundary edges of the triangulation \mathcal{T}_Ω , respectively. Moreover, \mathcal{N}_Γ equals the set of nodes of \mathcal{T}_Γ and $[\cdot]_E$ the jump along an edge E .

Making use of the mentioned Galerkin orthogonality, namely

$$B([u - u_h, p - p_h, \lambda - \lambda_h], [v_h, q_h, \mu_h]) = 0$$

for all $[v_h, q_h, \mu_h] \in \mathbb{X}_h$, we can add arbitrary discrete test functions. Hence, including $v_h \in \mathbb{V}_h$ as any quasi-interpolant of v (such as the Clément interpolant [Clé75]) and $q_h \in \mathbb{Q}_h$ as the (pointwise) interpolant of q , we can estimate

$$\begin{aligned} & B([u - u_h, p - p_h, \lambda - \lambda_h], [v, q, \mu]) \\ &= B([u - u_h, p - p_h, \lambda - \lambda_h], [v - v_h, q - q_h, \mu]) \end{aligned}$$

$$\begin{aligned}
&\leq \sum_{T \in \mathcal{T}_\Omega} \|f - \sigma u_h + \Delta_\alpha u_h\|_{L^2(T)} \|v - v_h\|_{L^2(T)} + \sum_{E \in \mathcal{E}_\Omega^{\text{in}}} \|[\alpha \nabla u_h \cdot n_E]_E\|_{L^2(E)} \|v - v_h\|_{L^2(E)} \\
&\quad + \sum_{E \in \mathcal{E}_\Omega^{\text{bd}}} \|\lambda_h - \alpha \nabla u_h \cdot n_E\|_{L^2(E)} \|v - v_h\|_{L^2(E)} \\
&\quad + \sum_{I \in \mathcal{T}_\Gamma} \|g - \sigma p_h + \Delta_{\Gamma, \kappa} p_h - \lambda_h\|_{L^2(I)} \|q - q_h\|_{L^2(I)} \\
&\quad + \sum_{x \in \mathcal{N}_\Gamma} |[\kappa \nabla_\Gamma p_h]_x| \underbrace{|q(x) - q_h(x)|}_{=0} + \|u_h - p_h\|_{H^{1/2}(\Gamma)} \|\mu\|_{H^{-1/2}(\Gamma)} \\
&\lesssim \sum_{T \in \mathcal{T}_\Omega} h_T \|f - \sigma u_h + \Delta_\alpha u_h\|_{L^2(T)} \|v\|_{H^1(\omega_T)} + \sum_{E \in \mathcal{E}_\Omega^{\text{in}}} h_E^{1/2} \|[\alpha \nabla u_h \cdot n_E]_E\|_{L^2(E)} \|v\|_{H^1(\omega_E)} \\
&\quad + \sum_{E \in \mathcal{E}_\Omega^{\text{bd}}} h_E^{1/2} \|\lambda_h - \alpha \nabla u_h \cdot n_E\|_{L^2(E)} \|v\|_{H^1(\omega_E)} \\
&\quad + \sum_{I \in \mathcal{T}_\Gamma} h_I \|g - \sigma p_h + \Delta_{\Gamma, \kappa} p_h - \lambda_h\|_{L^2(I)} \|q\|_{H^1(I)} + \|u_h - p_h\|_{H^{1/2}(\Gamma)} \|\mu\|_{H^{-1/2}(\Gamma)} \\
&\lesssim \left(\sum_{T \in \mathcal{T}_\Omega} h_T^2 \|f - \sigma u_h + \Delta_\alpha u_h\|_{L^2(T)}^2 + \sum_{E \in \mathcal{E}_\Omega^{\text{in}}} h_E \|[\alpha \nabla u_h \cdot n_E]_E\|_{L^2(E)}^2 \right. \\
&\quad + \sum_{E \in \mathcal{E}_\Omega^{\text{bd}}} h_E \|\lambda_h - \alpha \nabla u_h \cdot n_E\|_{L^2(E)}^2 + \sum_{I \in \mathcal{T}_\Gamma} h_I^2 \|g - \sigma p_h + \Delta_{\Gamma, \kappa} p_h - \lambda_h\|_{L^2(I)}^2 \\
&\quad \left. + \|u_h - p_h\|_{H^{1/2}(\Gamma)}^2 \right)^{1/2} \| [v, q, \mu] \|.
\end{aligned}$$

Here, we have used standard (quasi) interpolation results as presented, e.g., in [Car06]. This includes the well-known element and edge patches, denoted by ω_T and ω_E , respectively. Further note that the difference $u_h - p_h$ occurs globally, since the $H^{1/2}(\Gamma)$ -norm is not additive. For a local version, we use that \mathcal{T}_Γ is a refinement of $\mathcal{T}_\Omega|_\Gamma$. Thus, we can apply the interpolation inequality for $H^{1/2}(\Gamma)$, see [LM72, Ch.1 Prop. 2.3] and [AF03, p. 250 ff.], and the inverse estimate [Bra07, Ch. II.6.8]. Together with the Poincaré inequality, this leads to

$$\begin{aligned}
(3.2) \quad \|u_h - p_h\|_{H^{1/2}(\Gamma)}^2 &\lesssim \|u_h - p_h\|_{H^1(\Gamma)} \cdot \|u_h - p_h\|_{L^2(\Gamma)} \\
&\lesssim |u_h - p_h|_{H^1(\Gamma)} \cdot \|u_h - p_h\|_{L^2(\Gamma)} \\
&\lesssim \left(\sum_{I \in \mathcal{T}_\Gamma} h_I^{-2} \|u_h - p_h\|_{L^2(I)}^2 \cdot \sum_{I \in \mathcal{T}_\Gamma} \|u_h - p_h\|_{L^2(I)}^2 \right)^{1/2} \\
&\leq \left(\frac{h_{\Gamma, \max}}{h_{\Gamma, \min}} \right)^{1/2} \sum_{I \in \mathcal{T}_\Gamma} h_I^{-1} \|u_h - p_h\|_{L^2(I)}^2
\end{aligned}$$

with a hidden constant only depending on Γ and the polynomial degrees of \mathbb{V}_h and \mathbb{Q}_h . Here, $h_{\Gamma, \max}$ (respectively $h_{\Gamma, \min}$) denotes the maximal (minimal) mesh width of the triangulation \mathcal{T}_Γ ; see also Remark 3.5 below.

Finally, we define the following local quantities, which will serve as local error estimators, namely

$$(3.3a) \quad \eta_T^2 := h_T^2 \|f - \sigma u_h + \Delta_\alpha u_h\|_{L^2(T)}^2 \quad \text{for } T \in \mathcal{T}_\Omega,$$

$$(3.3b) \quad \eta_E^2 := h_E \left\| [\alpha \nabla u_h \cdot n_E]_E \right\|_{L^2(E)}^2 \quad \text{for } E \in \mathcal{E}_\Omega^{\text{in}},$$

$$(3.3c) \quad \eta_E^2 := h_E \left\| \lambda_h - \alpha \nabla u_h \cdot n_E \right\|_{L^2(E)}^2 + \sum_{I \in \mathcal{T}_\Gamma, I \subseteq E} h_I^{-1} \|u_h - p_h\|_{L^2(I)}^2 \quad \text{for } E \in \mathcal{E}_\Omega^{\text{bd}},$$

$$(3.3d) \quad \eta_I^2 := h_I^2 \|g - \sigma p_h + \Delta_{\Gamma, \kappa} p_h - \lambda_h\|_{L^2(I)}^2 \quad \text{for } I \in \mathcal{T}_\Gamma.$$

The remainder of this section is devoted to the verification of the reliability and efficiency of these estimators.

Remark 3.3. In the above derivation of the error estimators, we have used that functions in $H^1(\Gamma)$ are continuous for a one-dimensional boundary Γ of a two-dimensional domain Ω . This allows us to neglect the jumps of p over the nodes of \mathcal{T}_Γ . If Ω is a subset of \mathbb{R}^3 , however, we have to consider these jumps, which are now jumps over edges. As a consequence, the estimators in (3.3) need to be extended by

$$(3.4) \quad \eta_D^2 := h_D \left\| [\kappa \nabla_\Gamma p_h \cdot n_D]_D \right\|_{L^2(D)}^2 \quad \text{for } D \in \mathcal{E}_\Gamma$$

with \mathcal{E}_Γ being the set of edges of \mathcal{T}_Γ and h_D the length of an edge $D \in \mathcal{E}_\Gamma$.

3.2. Reliability and efficiency. The reliability of the introduced a posteriori estimators follows directly by construction and is summarized in the following theorem.

Theorem 3.4 (Reliability of the error estimator). *Let η_T , η_E , and η_I be defined as in (3.3) and let Assumption 3.1 be satisfied. Then the discretization error can be bounded by*

$$\begin{aligned} \|[u - u_h, p - p_h, \lambda - \lambda_h]\|^2 &= \|u - u_h\|_{H^1(\Omega)}^2 + \|p - p_h\|_{H^1(\Gamma)}^2 + \|\lambda - \lambda_h\|_{H^{-1/2}(\Gamma)}^2 \\ &\lesssim \sum_{T \in \mathcal{T}_\Omega} \eta_T^2 + \sum_{E \in \mathcal{E}_\Omega} \eta_E^2 + \sum_{I \in \mathcal{T}_\Gamma} \eta_I^2, \end{aligned}$$

where the hidden constant only depends on the dimension d , the polynomial degrees used for the finite element spaces, the domain Ω with its boundary Γ , and the shape regularity of the triangulations \mathcal{T}_Ω and \mathcal{T}_Γ , and the coefficients α , κ , and σ .

Remark 3.5. The calculation (3.2) shows that the hidden constant contains the ratio $h_{\Gamma, \max}/h_{\Gamma, \min}$, which may be large due to adaptive refinements. An alternative estimate of $u_h - p_h$ on Γ allows to replace this ratio by a constant which is independent of the mesh widths of \mathcal{T}_Γ and \mathcal{T}_Ω ; cf. [Lip04, Lem. 2.4.6]. For this, assume the use of bisection for $d = 2$ or newest vertex bisection for $d = 3$ to obtain \mathcal{T}_Γ . Then, there exists a refinement $\tilde{\mathcal{T}}_\Omega$ of \mathcal{T}_Ω such that $\mathcal{T}_\Gamma = \tilde{\mathcal{T}}_\Omega|_\Gamma$. Moreover, the shape regularity of $\tilde{\mathcal{T}}_\Omega$ only depends on \mathcal{T}_Ω and the dimension d ; see [DS11, Sect. A.1].

Remark 3.6. The reliability in the three-dimensional case follows similarly to Theorem 3.4, where we have the additional term $\sum_{D \in \mathcal{E}_\Gamma} \eta_D^2$ on the right-hand side, cf. Remark 3.3.

Theorem 3.4 guarantees that the error estimators provide an upper bound of the error. It remains to prove the efficiency of the estimators, i.e., the guarantee that they are (up to a constant) also a lower bound.

In the following lemmas, we always assume that Assumption 3.1 is satisfied. Similar to Theorem 3.4, all hidden constants will only depend on the dimension, the polynomial degrees of the finite element spaces, the domain with its boundary, the shape regularity of the meshes, the diffusion coefficients, and the constant ρ . We first consider the estimators η_T and η_I .

Lemma 3.7. *The estimators η_T and η_I satisfy*

$$(3.5a) \quad \eta_T^2 \lesssim \sigma^2 h_T^2 \|u - u_h\|_{L^2(T)}^2 + \|\alpha\|_{L^\infty(T)}^2 |u - u_h|_{H^1(T)}^2 + h_T^2 \inf_{f_h \in \mathbb{V}_h} \|f - f_h\|_{L^2(T)}^2$$

as well as

$$(3.5b) \quad \eta_I^2 \lesssim \sigma^2 h_I^2 \|p - p_h\|_{L^2(I)}^2 + \|\kappa\|_{L^\infty(I)}^2 |p - p_h|_{H^1(I)}^2 + h_I \|\lambda - \lambda_h\|_{H^{-1/2}(I)}^2 + h_I^2 \inf_{g_h \in \mathbb{Q}_h} \|g - g_h\|_{L^2(I)}^2.$$

These estimates further imply

$$(3.6a) \quad \sum_{T \in \mathcal{T}_\Omega} \eta_T^2 \lesssim \|u - u_h\|_{H^1(\Omega)}^2 + \sum_{T \in \mathcal{T}_\Omega} h_T^2 \inf_{f_h \in \mathbb{V}_h} \|f - f_h\|_{L^2(T)}^2,$$

$$(3.6b) \quad \sum_{I \in \mathcal{T}_\Gamma} \eta_I^2 \lesssim \|p - p_h\|_{H^1(\Gamma)}^2 + h_{\Gamma, \max} \|\lambda - \lambda_h\|_{H^{-1/2}(\Gamma)}^2 + \sum_{I \in \mathcal{T}_\Gamma} h_I^2 \inf_{g_h \in \mathbb{Q}_h} \|g - g_h\|_{L^2(I)}^2.$$

Proof. Estimate (3.5a) follows by the lines of [Lip04, Lem. 2.6.10(1)]. For (3.5b), we note that every segment $I \in \mathcal{T}_\Gamma$ is a part of a hyperplane $\mathbb{H}_I \cong \mathbb{R}^{d-1}$. With this, one proves (3.5b) analogously to (3.5a), where one uses that for every $\nu \in H_0^1(I)$ – extended by zero outside of I – it holds the interpolation inequality

$$\begin{aligned} \|\nu\|_{H^{1/2}(I)}^2 &= \int_I \nu(x)^2 dx + \int_I \int_I \frac{|\nu(x) - \nu(y)|^2}{\|x - y\|_{\mathbb{R}^d}^d} dx dy \\ &\leq \int_{\mathbb{H}_I} \nu(x)^2 dx + \int_{\mathbb{H}_I} \int_{\mathbb{H}_I} \frac{|\nu(x) - \nu(y)|^2}{\|x - y\|_{\mathbb{R}^d}^d} dx dy \\ &= \|\nu\|_{H^{1/2}(\mathbb{R}^{d-1})}^2 \lesssim \|\nu\|_{H^1(\mathbb{R}^{d-1})} \|\nu\|_{L^2(\mathbb{R}^{d-1})} = \|\nu\|_{H^1(I)} \|\nu\|_{L^2(I)}, \end{aligned}$$

see [LM72, Ch.1 Prop. 2.3 & Th. 7.1]. Inequality (3.6a) is a immediate consequence of (3.5a) together with $h_T \leq |\Omega|$. Finally, (3.6b) can be shown in the same manner as (3.5b) if adjusted to the entire boundary Γ . \square

To obtain an upper bound on η_E , we distinguish interior and boundary edges.

Lemma 3.8. *For an interior edge $E \in \mathcal{E}_\Omega^{\text{in}}$ it holds that*

$$\eta_E^2 \lesssim \sigma^2 h_E^2 \|u - u_h\|_{L^2(\omega_E)}^2 + \|\alpha\|_{L^\infty(\omega_E)}^2 |u - u_h|_{H^1(\omega_E)}^2 + \sum_{T \in \mathcal{T}_\Omega, T \subseteq \omega_E} \eta_T^2$$

and, hence,

$$\sum_{E \in \mathcal{E}_\Omega^{\text{in}}} \eta_E^2 \lesssim \|u - u_h\|_{H^1(\Omega)}^2 + \sum_{T \in \mathcal{T}_\Omega} h_T^2 \inf_{f_h \in \mathbb{V}_h} \|f - f_h\|_{L^2(T)}^2.$$

Proof. The proof follows the lines of [AO97, Lem. 3.6]. \square

Lemma 3.9. *For a boundary edge $E \in \mathcal{E}_\Omega^{\text{bd}}$ we define the boundary edge patch $\omega_{E,\Gamma}$ by*

$$\omega_{E,\Gamma} := \{E' \in \mathcal{E}_\Omega^{\text{bd}} \mid \overline{E} \cap \overline{E'} \neq \emptyset\}$$

and T_E as the (unique) element in \mathcal{T}_Ω with edge E . Then, it holds that

$$\eta_E^2 \lesssim \|u - u_h\|_{H^1(\omega_{T_E})}^2 + \|p - p_h\|_{H^1(\omega_{E,\Gamma})}^2 + h_E^{1/2} \|\lambda - \lambda_h\|_{H^{-1/2}(E)}^2 + h_{T_E}^2 \inf_{f_h \in \mathbb{V}_h} \|f - f_h\|_{L^2(T_E)}^2$$

and, hence,

$$\sum_{E \in \mathcal{E}_\Omega^{\text{bd}}} \eta_E^2 \lesssim \|u - u_h\|_{H^1(\Omega)}^2 + \|p - p_h\|_{H^1(\Gamma)}^2 + \|\lambda - \lambda_h\|_{H^{-1/2}(\Gamma)}^2 + \sum_{E \in \mathcal{E}_\Omega^{\text{bd}}} h_{T_E}^2 \inf_{f_h \in \mathbb{V}_h} \|f - f_h\|_{L^2(T_E)}^2.$$

Proof. Combining the arguments of [Lip04, Lem. 2.6.12], [AO97, Lem. 3.6], and the one used for the derivation of (3.5b), we have

$$\begin{aligned} h_E \|\lambda_h - \alpha \nabla u_h \cdot n_E\|_{L^2(E)}^2 &\lesssim \sigma^2 h_E^2 \|u - u_h\|_{L^2(T_E)}^2 + \|\alpha\|_{L^\infty(T_E)}^2 \|u - u_h\|_{H^1(T_E)}^2 \\ &\quad + h_E^{1/2} \|\lambda - \lambda_h\|_{H^{-1/2}(E)}^2 + \eta_{T_E}^2 \end{aligned}$$

and, hence, for the entire boundary

$$\sum_{E \in \mathcal{E}_\Omega^{\text{bd}}} h_E \|\lambda_h - \alpha \nabla u_h \cdot n_E\|_{L^2(E)}^2 \lesssim \|u - u_h\|_{H^1(\Omega)}^2 + \|\lambda - \lambda_h\|_{H^{-1/2}(\Gamma)}^2 + \sum_{E \in \mathcal{E}_\Omega^{\text{bd}}} \eta_{T_E}^2.$$

For an estimate of the second summand of η_E , we set $\mu := \sum_{I \in \mathcal{T}_\Gamma, I \subseteq E} h_I^{-1} (u_h - p_h) \chi_I \in L^2(\Gamma) \hookrightarrow H^{-1/2}(\Gamma)$ with the characteristic function χ_I . We now distinguish the two cases $\mathcal{P}_0^d(\mathcal{T}_\Omega|\Gamma) \subseteq \mathbb{M}_h$ and $\mathcal{P}_1(\mathcal{T}_\Omega|\Gamma) \subseteq \mathbb{M}_h$, cf. Assumption 3.1(1).

Case $\mathcal{P}_0^d(\mathcal{T}_\Omega|\Gamma) \subseteq \mathbb{M}_h$: If piecewise constant functions are part of \mathbb{M}_h , we define the mean integral of μ as $\mu_h := \frac{1}{|E|} \int_E \mu \, dx \cdot \chi_E \in \mathbb{M}_h$. Then, the continuous and discrete constraint imply that

$$\begin{aligned} \sum_{I \in \mathcal{T}_\Gamma, I \subseteq E} h_I^{-1} \|u_h - p_h\|_{L^2(I)}^2 &= \int_E \mu (u_h - p_h) \, dx \\ &= \int_E (\mu - \mu_h) (u_h - u - (p_h - p)) \, dx \\ &\leq \|\mu - \mu_h\|_{H^{-1/2}(E)} (\|u - u_h\|_{H^{1/2}(E)} + \|p - p_h\|_{H^{1/2}(E)}). \end{aligned}$$

By [AB17, Prop. 2.2 & 4.8], there exists a constant only depending on the shape regularity of $\mathcal{T}_\Omega|\Gamma$ such that

$$\begin{aligned} \|\mu - \mu_h\|_{H^{-1/2}(E)} &= \sup_{q \in H^{1/2}(E) \setminus \{0\}} \frac{(\mu - \mu_h, q)_{L^2(E)}}{\|q\|_{H^{1/2}(E)}} \\ &= \sup_{q \in H^{1/2}(E) \setminus \{0\}} \frac{(\mu, q - \frac{1}{|E|} \int_E q \, dx)_{L^2(E)}}{\|q\|_{H^{1/2}(E)}} \\ &\lesssim h_E^{1/2} \|\mu\|_{L^2(E)} \leq \sqrt{\rho} \left(\sum_{I \in \mathcal{T}_\Gamma, I \subseteq E} h_I^{-1} \|u_h - p_h\|_{L^2(I)}^2 \right)^{1/2}. \end{aligned}$$

Combining the latter two estimates, we conclude that

$$\sum_{I \in \mathcal{T}_\Gamma, I \subseteq E} h_I^{-1} \|u_h - p_h\|_{L^2(I)}^2 \lesssim \|u - u_h\|_{H^{1/2}(E)}^2 + \|p - p_h\|_{H^{1/2}(E)}^2.$$

With Lemma 3.7 and appropriate Sobolev embeddings, we get the stated estimate for η_E . Finally, the estimate of the sum follows by $\sum_{E \in \mathcal{E}_\Omega^{\text{bd}}} \|\cdot\|_{H^{1/2}(E)}^2 \leq \|\cdot\|_{H^{1/2}(\Gamma)}^2$.

Case $\mathcal{P}_1(\mathcal{T}_\Omega|_\Gamma) \subseteq \mathbb{M}_h$: Let $P_E: L^2(\omega_{E,\Gamma}) \rightarrow \mathcal{P}_1(\mathcal{T}_\Omega|_{\omega_{E,\Gamma}}) \subseteq H^1(\omega_{E,\Gamma})$ be the (weighted) Clément operator

$$P_E r = \sum_{k=1}^m \frac{(r, \phi_k)_{L^2(\omega_{E,\Gamma})}}{(1, \phi_k)_{L^2(\omega_{E,\Gamma})}} \phi_k$$

with the nodal basis functions ϕ_k , $k = 1, \dots, m$, of $\mathcal{P}_1(\mathcal{T}_\Omega|_{\omega_{E,\Gamma}})$. Since μ vanishes outside of E , its quasi-interpolation $P_E \mu$ is zero on the relative boundary $\partial\omega_{E,\Gamma}$. Hence, $P_E \mu$ can be extended by zero to a function in \mathbb{M}_h . Similar to the previous case, we obtain the estimate

$$\sum_{I \in \mathcal{T}_\Gamma, I \subseteq E} h_I^{-1} \|u_h - p_h\|_{L^2(I)}^2 \leq \|\mu - P_E \mu\|_{H^{-1/2}(\omega_{E,\Gamma})} (\|u - u_h\|_{H^{1/2}(\omega_{E,\Gamma})} + \|p - p_h\|_{H^{1/2}(\omega_{E,\Gamma})}).$$

By [BPV00, Lem. 3.1], we have $\|\mu - P_E \mu\|_{L^2(\omega_{E,\Gamma})} \lesssim \|\mu\|_{L^2(E)}$ as well as

$$\|\mu - P_E \mu\|_{[H^1(\omega_{E,\Gamma})]^*} = \sup_{q \in H^1(E) \setminus \{0\}} \frac{(\mu, q - P_E q)_{L^2(E)}}{\|q\|_{H^1(\omega_{E,\Gamma})}} \lesssim h_E \|\mu\|_{L^2(E)}$$

with constants only depending on the regularity of $\mathcal{T}_\Omega|_\Gamma$. Here, we have used that P_E is symmetric with respect to the $L^2(\omega_{E,\Gamma})$ -inner product. With the interpolation inequality we conclude $\|\mu - P_E \mu\|_{H^{-1/2}(\omega_{E,\Gamma})} \lesssim h_E^{1/2} \|\mu\|_{L^2(E)}$. The remainder of the proof follows the lines of the first case. \square

It remains to summarize the previous estimates. The combination of Lemmas 3.7, 3.8, and 3.9 yield the following efficiency result, showing that the error estimators are bounded from above by the actual error plus oscillation terms of the right-hand sides.

Theorem 3.10 (Efficiency of the error estimator). *Given Assumption 3.1, the error estimators defined in (3.3) satisfy*

$$\begin{aligned} & \sum_{T \in \mathcal{T}_\Omega} \eta_T^2 + \sum_{E \in \mathcal{E}_\Omega} \eta_E^2 + \sum_{I \in \mathcal{T}_\Gamma} \eta_I^2 \\ & \lesssim \|u - u_h\|_{H^1(\Omega)}^2 + \|p - p_h\|_{H^1(\Gamma)}^2 + \|\lambda - \lambda_h\|_{H^{-1/2}(\Gamma)}^2 \\ & \quad + \sum_{T \in \mathcal{T}_\Omega} h_T^2 \inf_{f_h \in \mathbb{V}_h} \|f - f_h\|_{L^2(T)}^2 + \sum_{I \in \mathcal{T}_\Gamma} h_I^2 \inf_{g_h \in \mathbb{Q}_h} \|g - g_h\|_{L^2(I)}^2 \\ & = \|[u - u_h, p - p_h, \lambda - \lambda_h]\|^2 + \sum_{T \in \mathcal{T}_\Omega} h_T^2 \inf_{f_h \in \mathbb{V}_h} \|f - f_h\|_{L^2(T)}^2 + \sum_{I \in \mathcal{T}_\Gamma} h_I^2 \inf_{g_h \in \mathbb{Q}_h} \|g - g_h\|_{L^2(I)}^2. \end{aligned}$$

The hidden constant only depends on the dimension d , the polynomial degrees of the finite element spaces, the domain Ω with its boundary Γ , the shape regularity of the triangulations \mathcal{T}_Ω and \mathcal{T}_Γ , the coefficients α and κ , as well as the constants σ and ρ .

Remark 3.11. Analogously to η_E in Lemma 3.8, the additional error estimator η_D defined in (3.4) is bounded by

$$\eta_D^2 \lesssim \sigma^2 h_D^2 \|p - p_h\|_{L^2(\omega_D)}^2 + \|\kappa\|_{L^\infty(\omega_D)}^2 \|p - p_h\|_{H^1(\omega_D)}^2 + \sum_{I \in \mathcal{T}_\Gamma, I \subseteq \omega_D} \eta_I^2$$

for a three-dimensional domain Ω . Here, ω_D is defined with respect to \mathcal{T}_Γ as ω_E to \mathcal{T}_Ω . Furthermore, Lemmas 3.7, 3.8, and 3.9 are also valid for $\Omega \subseteq \mathbb{R}^3$, implicating again the efficiency of the error estimators.

4. NUMERICAL EXPERIMENTS

In this final section, we demonstrate the performance of the newly introduced a posteriori error estimators applied to the stationary model problem (2.3) as well as a parabolic problem with dynamic boundary conditions.

In all examples, we consider a two-dimensional domain and diffusion coefficients $\alpha \equiv 1$, $\kappa \equiv 1$. Moreover, we use bisection as refinement strategy for \mathcal{T}_Γ and newest vertex bisection for \mathcal{T}_Ω with the implementation taken from [FPW11]. Since newest vertex bisection is based on element marking (instead of marking elements and edges), we attribute the estimator η_E of an edge E among all η_T and η_I with $T \subseteq \omega_E$ and $I \subseteq E$, respectively. The resulting error estimators are denoted by $\tilde{\eta}_T$ and $\tilde{\eta}_I$. As marking strategy, we use the well-known *Dörfler marking* with a parameter $\theta \in (0, 1)$, i.e., we mark all elements in (minimal) sets $\mathcal{M}_\Omega \subseteq \mathcal{T}_\Omega$ and $\mathcal{M}_\Gamma \subseteq \mathcal{T}_\Gamma$ such that

$$(1 - \theta) \left(\sum_{T \in \mathcal{T}_\Omega} \tilde{\eta}_T^2 + \sum_{I \in \mathcal{T}_\Gamma} \tilde{\eta}_I^2 \right) \leq \sum_{T \in \mathcal{M}_\Omega} \tilde{\eta}_T^2 + \sum_{I \in \mathcal{M}_\Gamma} \tilde{\eta}_I^2.$$

For the computation of the errors, we use a reference solution, which is computed on a refined mesh. More precisely, we consider in each step the current mesh obtained by the adaptive process with two additional uniform refinements.

4.1. Stationary problem on the unit square. In this first example, we consider the stationary model problem (2.3) on the unit square, i.e., on $\Omega = (0, 1)^2$. The right-hand sides are given by

$$f \equiv 0.04, \quad g(x, y) = xy \cos(10\pi x) \cos(10\pi y)$$

and we set $\sigma = 1$ as well as $\theta = 0.75$ for the marking process. The resulting convergence history for the scheme

$$(4.1) \quad \mathbb{V}_h = \mathcal{P}_1(\mathcal{T}_\Omega), \quad \mathbb{Q}_h = \mathcal{P}_1(\mathcal{T}_\Gamma), \quad \mathbb{M}_h = \mathcal{P}_1(\mathcal{T}_\Omega|_\Gamma)$$

is illustrated in Figure 4.1. Note that the x -axis includes the sum of the degrees of freedom for u , p , and λ . The plot clearly shows the improvement caused by the adaptive process as we reach a convergence rate of 0.65 rather than 0.5 for a uniform refinement. Moreover, one can observe that error and estimator, which are defined as

$$\text{error} := \|[u - u_h, p - p_h, \lambda - \lambda_h]\|, \quad \text{estimator} := \left(\sum_{T \in \mathcal{T}_\Omega} \eta_T^2 + \sum_{E \in \mathcal{E}_\Omega} \eta_E^2 + \sum_{I \in \mathcal{T}_\Gamma} \eta_I^2 \right)^{1/2}$$

are indeed of the same order as expected due to Theorems 3.4 and 3.10.

The resulting mesh of the adaptive process is shown in Figure 4.2. It clearly shows a refinement of the upper right corner for \mathcal{T}_Ω as well as for \mathcal{T}_Γ . This is due to the fact that the right-hand side g as well as the solution oscillate strongly in this region.

4.2. Stationary problem on the L-shape. The second example works on the L-shape, i.e., on a non-convex computational domain. Here, we consider the right-hand sides

$$f \equiv 4, \quad g(x, y) = 4(x^2 - x + y^2 - y)$$

and again $\sigma = 1$, $\theta = 0.75$. We compare two different stable finite element schemes.

First, we use piecewise linear elements as in (4.1). As shown in Figure 4.3, this yields the rate 0.375 for a uniform refinement and the optimal rate 0.5 in the adaptive case.

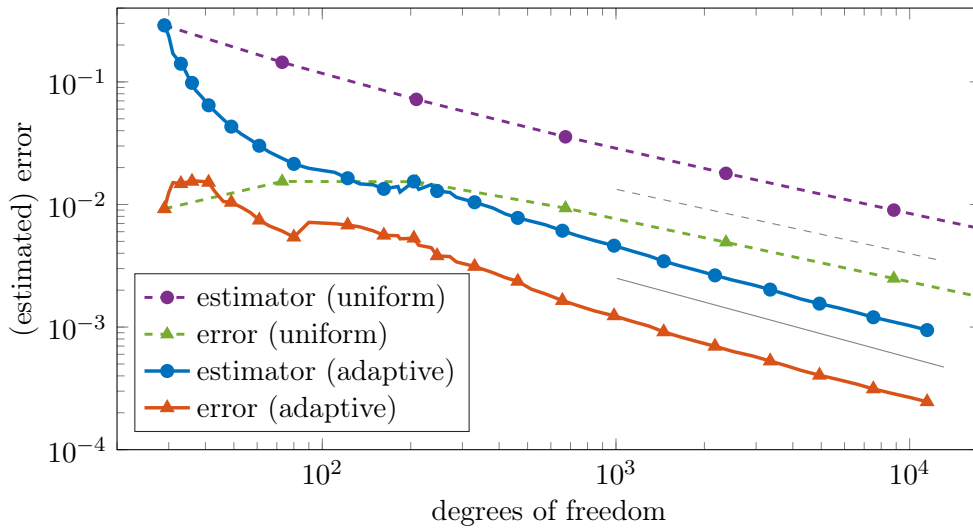


FIGURE 4.1. Convergence history for the stationary model problem of Section 4.1. The dashed line in gray indicates order 0.525 (for a uniform refinement), whereas the solid gray line indicates order 0.65.

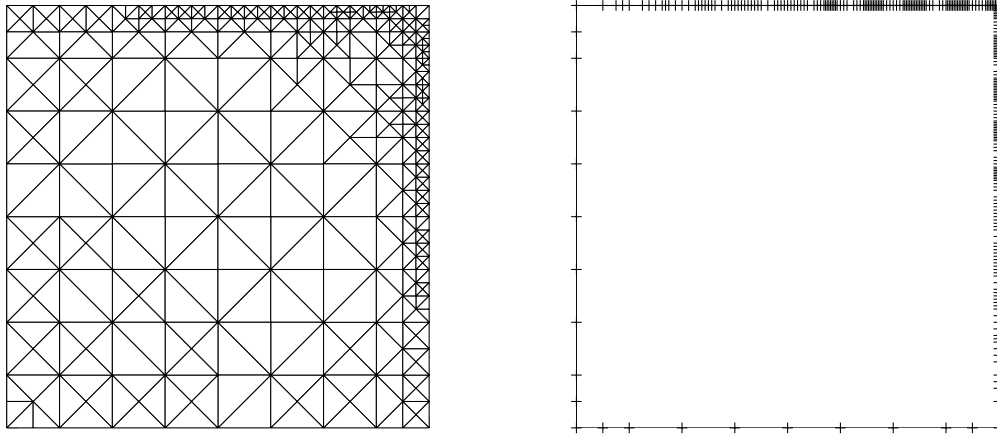


FIGURE 4.2. Illustration of the bulk mesh \mathcal{T}_Ω (left) and the boundary mesh \mathcal{T}_Γ (right) after 40 adaptive refinement steps.

Second, we consider a piecewise quadratic approximation for u and p in combination with a piecewise constant approximation of the Lagrange multiplier, i.e.,

$$(4.2) \quad \mathbb{V}_h = \mathcal{P}_2(\mathcal{T}_\Omega), \quad \mathbb{Q}_h = \mathcal{P}_2(\mathcal{T}_\Gamma), \quad \mathbb{M}_h = \mathcal{P}_0^d(\mathcal{T}_\Omega|_\Gamma).$$

Note that this is indeed a stable scheme according to the derivations of Section 2.3. The convergence results are shown in Figure 4.4 and demonstrate an even higher numerical gain of the adaptive procedure. If the discrete multiplier space \mathbb{M}_h is set to $\mathcal{P}_1(\mathcal{T}_\Omega|_\Gamma)$

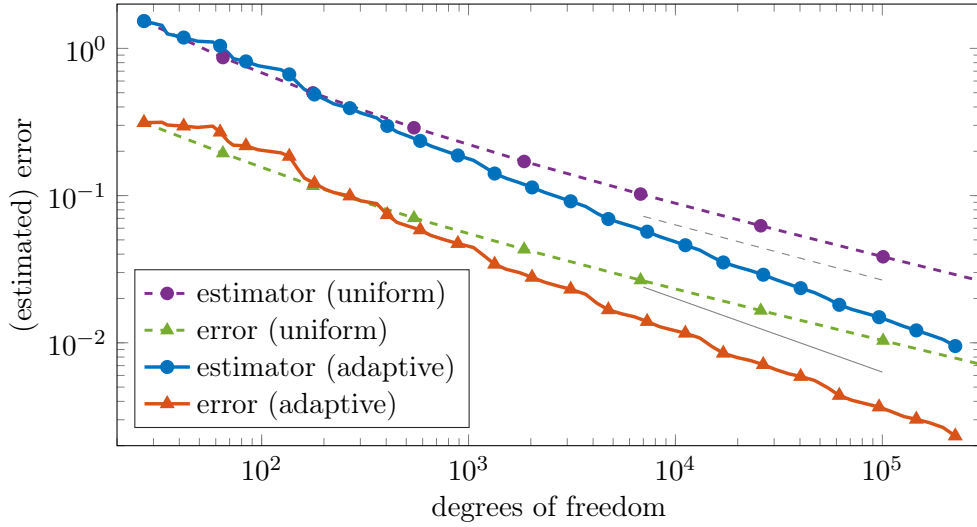


FIGURE 4.3. Convergence history for the stationary model problem of Section 4.2 using piecewise linear elements. The gray lines indicate orders 0.375 (dashed) and 0.5 (solid).

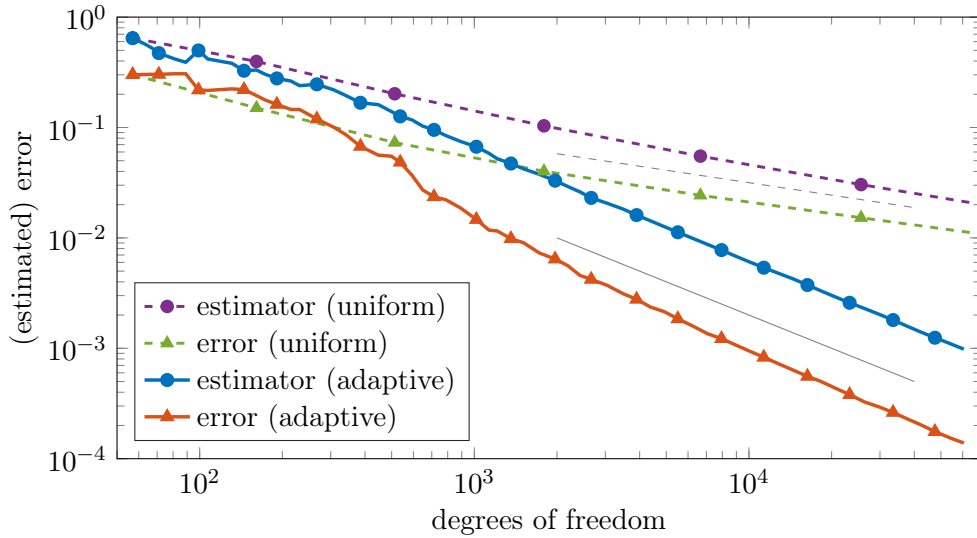


FIGURE 4.4. Convergence history for the stationary model problem of Section 4.2 using piecewise quadratic elements for u , p and piecewise constants for λ . The gray lines indicate orders 0.375 (dashed) and 1.0 (solid).

or $\mathcal{P}_2(\mathcal{T}_\Omega|_\Gamma)$, we observe the same rates. Hence, we omit the corresponding error plots here.

An illustration of the adaptive mesh refinement is given in Figure 4.5. Note that both meshes show refinements in the same regions. Nevertheless, u restricted to the boundary

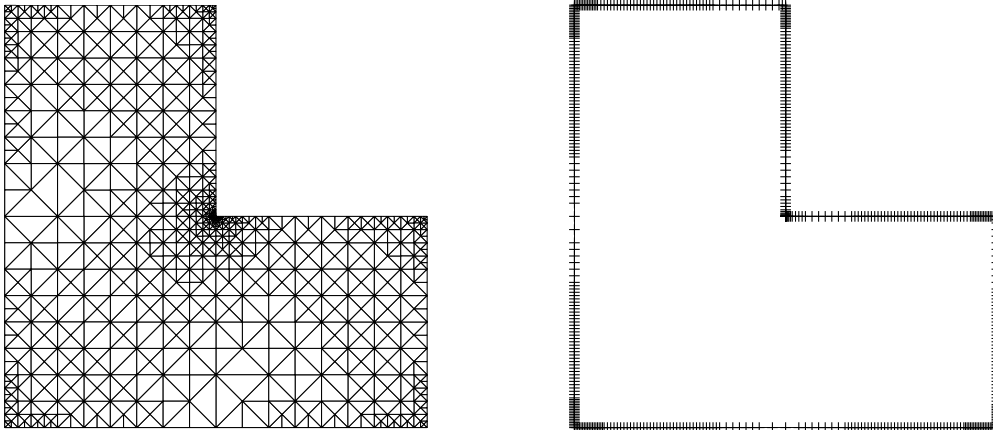


FIGURE 4.5. Illustration of the bulk mesh \mathcal{T}_Ω (left) and the boundary mesh \mathcal{T}_Γ (right) after 40 adaptive refinement steps.

has 190 degrees of freedom, whereas p is defined on a mesh with 1030 degrees of freedom. This additional refinement of the boundary is only possible because of the special formulation of the system equations as coupled system. Without the separation of $u|_\Gamma$ and p , we would need a refinement of $\mathcal{T}_\Omega|_\Gamma$ in order to get the same accuracy. This, however, would call for an significant increase of the degrees of freedom due to the higher topological dimension of the bulk.

4.3. Parabolic problem with dynamic boundary conditions. Within this final numerical example, we consider the dynamic problem

$$\begin{aligned} \dot{u} - \Delta u &= 0.1 && \text{in } \Omega = (0, 1)^2, \\ \dot{u} - \Delta_\Gamma u + \partial_n u &= xy \cos(\pi tx) \cos(\pi ty) && \text{on } \Gamma = \partial\Omega. \end{aligned}$$

with homogeneous initial data. For the computation, we set $[1, 10]$ as time horizon and apply the implicit Euler scheme with constant step size $\tau = 1.5 \cdot 10^{-2}$ for the time stepping. For the spatial discretization, we consider piecewise quadratic elements as in (4.2). At every time point, we check if the estimated spatial error is smaller than 10^{-6} . If not, we use the mentioned Dörfler marking strategy with parameter $\theta = 0.75$ and refine the meshes until this condition is satisfied. In the beginning, we start with 41, 16, and 8 degrees of freedom for u , p , and λ , respectively. At the end of the simulation, the numbers are 4912, 20674, and 301. The detailed development of the degrees of freedom over time is illustrated in Figure 4.6.

Finally, we present the approximated solution u at the final time point $t = 10$ in Figure 4.7. One can see that the solution is oscillating strongly at the boundary parts $(0, 1) \times \{1\}$ and $\{1\} \times (0, 1)$. To capture this behavior numerically, we need more degrees of freedom for p . On the other hand, the approximation of u gets along on a coarser mesh, since the solution is not so oscillatory in the bulk.

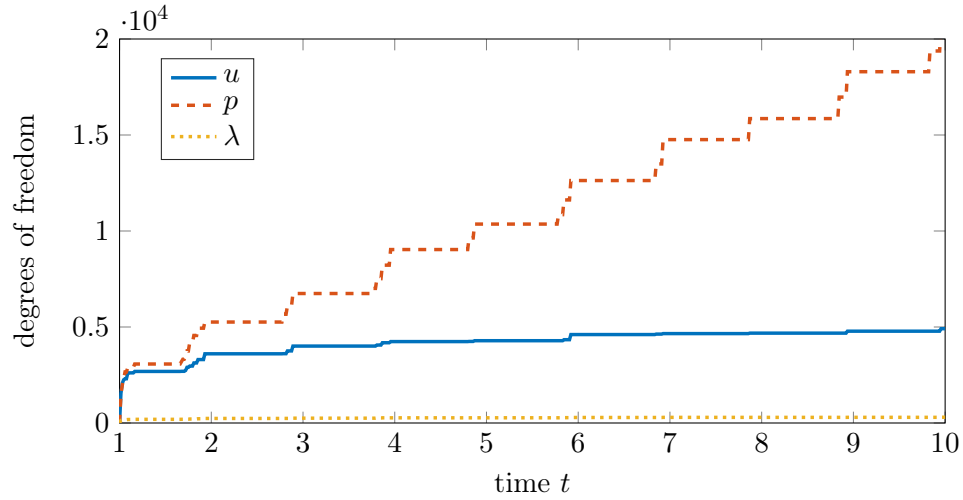


FIGURE 4.6. Evolution of the degrees of freedom for u , p , and λ over time.

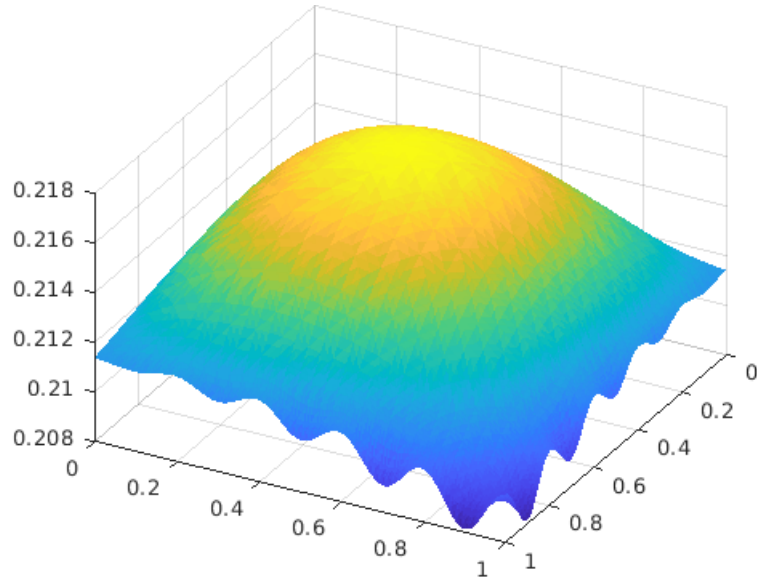


FIGURE 4.7. Numerical solution u at the final time point $T = 10$ for the parabolic problem of Section 4.3

5. CONCLUSION

In this paper, we have introduced an adaptive procedure for the simulation of parabolic problems with dynamic boundary conditions. Based on a PDAE formulation, we are able to construct local error estimators, which distinguish necessary refinements of the bulk mesh along the boundary, i.e., of $\mathcal{T}_\Omega|_\Gamma$, and the boundary mesh \mathcal{T}_Γ . Moreover, we have characterized inf-sup stable finite element schemes for the spatial discretization. Within

a number of numerical experiments, we have shown that the proposed algorithm reaches optimal convergence rates. In addition, one can observe that the boundary mesh gets more refined than $\overline{\mathcal{T}}_{\Omega}|_{\Gamma}$, which yields notable computational savings.

REFERENCES

- [AB17] G. Acosta and J. P. Borthagaray. A fractional Laplace equation: Regularity of solutions and finite element approximations. *SIAM J. Numer. Anal.*, 55(2):472–495, 2017.
- [AF03] R. A. Adams and J. J. F. Fournier. *Sobolev Spaces*. Elsevier/Academic Press, Amsterdam, second edition, 2003.
- [AKZ22] R. Altmann, B. Kovács, and C. Zimmer. Bulk–surface Lie splitting for parabolic problems with dynamic boundary conditions. *IMA J. Numer. Anal.*, published online, 2022.
- [Alt15] R. Altmann. *Regularization and Simulation of Constrained Partial Differential Equations*. PhD thesis, Technische Universität Berlin, 2015.
- [Alt19] R. Altmann. A PDAE formulation of parabolic problems with dynamic boundary conditions. *Appl. Math. Lett.*, 90:202–208, 2019.
- [AO97] M. Ainsworth and J. T. Oden. A posteriori error estimation in finite element analysis. *Comput. Methods Appl. Mech. Engrg.*, 142(1):1–88, 1997.
- [AV21] R. Altmann and B. Verfürth. A multiscale method for heterogeneous bulk–surface coupling. *Multiscale Model. Simul.*, 19(1):374–400, 2021.
- [AZ22a] R. Altmann and C. Zimmer. Dissipation-preserving discretization of the Cahn–Hilliard equation with dynamic boundary conditions. ArXiv Preprint 2203.15097, 2022.
- [AZ22b] R. Altmann and C. Zimmer. Second-order bulk–surface splitting for parabolic problems with dynamic boundary conditions. ArXiv Preprint 2209.07835, 2022.
- [BF91] F. Brezzi and M. Fortin. *Mixed and Hybrid Finite Element Methods*. Springer, New York, NY, 1991.
- [BPV00] J. H. Bramble, J. E. Pasciak, and P. S. Vassilevski. Computational scales of Sobolev norms with application to preconditioning. *Math. Comp.*, 69(230):463–480, 2000.
- [Bra07] D. Braess. *Finite Elements - Theory, Fast Solvers, and Applications in Solid Mechanics*. Cambridge University Press, New York, NY, third edition, 2007.
- [Car06] C. Carstensen. Clément interpolation and its role in adaptive finite element error control. In E. Koelink, J. van Neerven, B. de Pagter, G. Sweers, A. Luger, and H. Woracek, editors, *Partial Differential Equations and Functional Analysis: The Philippe Clément Festschrift*, pages 27–43, Basel, 2006. Birkhäuser Verlag, Basel.
- [CFK23] P. Csomós, B. Farkas, and B. Kovács. Error estimates for a splitting integrator for abstract semilinear boundary coupled systems. *IMA J. Numer. Anal.*, published online, 2023.
- [Clé75] P. Clément. Approximation by finite element functions using local regularization. *RAIRO Anal. Numér.*, 2:77–84, 1975.
- [DS11] A. Demlow and R. Stevenson. Convergence and quasi-optimality of an adaptive finite element method for controlling L_2 errors. *Numer. Math.*, 117:185–218, 2011.
- [Esc93] J. Escher. Quasilinear parabolic systems with dynamical boundary conditions. *Commun. Part. Diff. Eq.*, 18(7-8):1309–1364, 1993.
- [FGGR02] A. Favini, G. R. Goldstein, J. A. Goldstein, and S. Romanelli. The heat equation with generalized Wentzell boundary condition. *J. Evol. Equ.*, 2(1):1–19, 2002.
- [FPW11] S. Funken, D. Praetorius, and P. Wissgott. Efficient implementation of adaptive P1-FEM in Matlab. *Comput. Methods Appl. Math.*, 11(4):460–490, 2011.
- [GGZ74] H. Gajewski, K. Gröger, and K. Zacharias. *Nichtlineare Operatorgleichungen und Operatordifferential-Gleichungen*. Akademie-Verlag, Berlin, 1974.
- [Gol06] G. R. Goldstein. Derivation and physical interpretation of general boundary conditions. *Adv. Differential Equ.*, 11(4):457–480, 2006.
- [GT01] D. Gilbarg and N. S. Trudinger. *Elliptic Partial Differential Equations of Second Order*. Springer-Verlag, Berlin, 2001.
- [HLR89] E. Hairer, C. Lubich, and M. Roche. *The Numerical Solution of Differential-Algebraic Systems by Runge–Kutta Methods*. Springer-Verlag, Berlin, 1989.

- [HM12] R. Hiptmair and S. Mao. Stable multilevel splittings of boundary edge element spaces. *BIT Numer. Math.*, 52:661–685, 2012.
- [HW96] E. Hairer and G. Wanner. *Solving Ordinary Differential Equations II: Stiff and Differential-Algebraic Problems*. Springer-Verlag, Berlin, second edition, 1996.
- [KL17] B. Kovács and C. Lubich. Numerical analysis of parabolic problems with dynamic boundary conditions. *IMA J. Numer. Anal.*, 37(1):1–39, 2017.
- [Las02] I. Lasiecka. *Mathematical Control Theory of Coupled PDEs*. Society for Industrial and Applied Mathematics (SIAM), Philadelphia, PA, 2002.
- [Lip04] M. K. Lipinski. *A posteriori Fehlerschätzer für Sattelpunktsformulierungen nicht-homogener Randwertprobleme*. PhD thesis, Ruhr Universität Bochum, 2004.
- [LM72] J.-L. Lions and E. Magenes. *Non-Homogeneous Boundary Value Problems and Applications I*. Springer-Verlag, New York, NY, 1972.
- [LMT13] R. Lamour, R. März, and C. Tischendorf. *Differential-Algebraic Equations: A Projector Based Analysis*. Springer-Verlag, Berlin, Heidelberg, 2013.
- [LT85] P. Lancaster and M. Tismenetsky. *The Theory of Matrices: With Applications*. Academic Press, Inc., San Diego, CA, second edition, 1985.
- [LW19] C. Liu and H. Wu. An energetic variational approach for the Cahn–Hilliard equation with dynamic boundary condition: Model derivation and mathematical analysis. *Arch. Rational Mech. Anal.*, 233:167–247, 2019.
- [SZ90] L. R. Scott and S. Zhang. Finite element interpolation of nonsmooth functions satisfying boundary conditions. *Math. Comp.*, 54(190):483–493, 1990.
- [Tay11] M. E. Taylor. *Partial Differential Equations I: Basic Theory*. Springer, New York, NY, second edition, 2011.
- [Ver13] R. Verfürth. *A Posteriori Error Estimation Techniques for Finite Element Methods*. Oxford University Press, Oxford, 2013.
- [Vit18] E. Vitillaro. On the the wave equation with hyperbolic dynamical boundary conditions, interior and boundary damping and source. *J. Differ. Equations*, 265(10):4873–4941, 2018.
- [VS13] V. Vrábel’ and M. Slodička. Nonlinear parabolic equation with a dynamical boundary condition of diffusive type. *Appl. Math. Comput.*, 222:372–380, 2013.
- [VV08] J. L. Vázquez and E. Vitillaro. Heat equation with dynamical boundary conditions of reactive type. *Commun. Part. Diff. Eq.*, 33(4):561–612, 2008.
- [Zim21] C. Zimmer. *Temporal Discretization of Constrained Partial Differential Equations*. PhD thesis, Technische Universität Berlin, 2021.

† DEPARTMENT OF MATHEMATICS, UNIVERSITY OF AUGSBURG, UNIVERSITÄTSSTR. 14, 86159 AUGSBURG, GERMANY

Email address: robert.altmann@math.uni-augsburg.de, christoph.zimmer@math.uni-augsburg.de